

## CHARACTERISATION OF HEAT TRANSFER IN HIGH THERMAL CONDUCTIVITY GRAPHITE FOAM

Leong K.C. \*, Jin L.W., Chai J.C.

\*Author for correspondence

School of Mechanical and Aerospace Engineering,  
Nanyang Technological University  
50 Nanyang Avenue, Singapore 639798  
Republic of Singapore  
E-mail: mkcleong@ntu.edu.sg

### ABSTRACT

This paper presents the results of an experimental investigation of forced convection heat transfer in microcellular graphite foam of high thermal conductivity. The test section was designed to be adiabatic with constant heat flux supplied at the bottom of the channel. The graphite foam heat sinks were fabricated into different structures and compared with conventional aluminum heat sinks of the same configurations. Heat transfer characteristics including local temperature and Nusselt number distributions for steady flow through the tested heat sinks were measured and discussed. The results show that graphite foam heat sinks give better heat transfer performance as compared to conventional aluminum heat sinks for different configurations. The highest heat transfer rate is obtained by the graphite foam heat sink with a fin structure. The study implies that graphite foam material can offer a combination of properties ideally suited for applications in high heat flux thermal management applications where conventional materials and products are not adequate.

### INTRODUCTION

In recent decades, rapid development in the design of electronic packages for modern high-speed computers has led to the demand for new and reliable methods of chip cooling. Many techniques such as micro-channels, heat pipes and other exotic designs have been explored to improve the efficiencies of heat transfer devices [1, 2]. The primary concerns in thermal management applications are high thermal conductivity, large specific surface area and low weight. An effective method is to utilize a porous medium to enhance heat transfer by increasing the fluid-solid contact surface area and promoting fluid mixing. Metallic porous foams have been successfully used as heat exchangers for airborne equipment and compact heat sinks for power electronics [3-7]. A graphite foam which possesses predominantly spherical pores with smaller openings between the cells is a novel type of porous material with high thermal

conductivity. Fig. 1 shows the typical internal structure of high-conductivity carbon foam developed at Oak Ridge National Laboratory (ORNL) which possesses an open-cell structure with highly aligned graphitic ligaments. The thermal conductivities along the ligament are approximately 1700 W/m·K and bulk conductivities are around 180 W/m·K. Furthermore, the material exhibits low densities (0.25 to 0.6 g/cm<sup>3</sup>) which combined with the very large surface area to volume ratio (20,000 m<sup>2</sup>/m<sup>3</sup>) results in high overall heat transfer [8, 9]. Therefore, the bulk thermal conductivities are almost equivalent to dense aluminum alloys with only 1/5 the weight of solid aluminum material [10].

Attracted by the advantages of the graphite foam's thermal properties, some researchers have investigated the graphite foam in thermal management applications. Porous carbon foam fins were studied as a replacement for aluminum fins in finned tube radiators [11]. Their interest is driven by the notion that the unique thermodynamic properties of the foam would serve to reduce the thermal resistance of a heat exchanger without significant additional pressure drop. Yu *et al.* [12] presented an

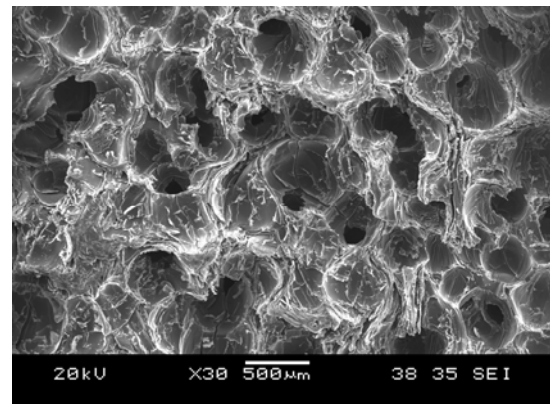


Fig. 1 Typical internal structure of graphite foam

engineering model to account for the effects of porosity and pore diameter on the hydrodynamic and thermal performance of a graphite foam finned tube heat exchanger. The parametric study suggests that in comparison to conventional aluminum finned tube radiators, improvements of approximately 15% in thermal performance are possible without changing the frontal area or the air flow rate and pressure drop. Druma *et al.* [13] performed a finite element analysis to calculate the thermal conductivity of graphite foam for the complete range of porosity and interpreted the results in terms of analytical and semi-empirical solutions. Coursey *et al.* [14] conducted an experimental study on the thermal performance of a graphite foam thermosyphon evaporator and discussed the foam's potential for use in the thermal management of electronics. They concluded that the use of graphite foam as the evaporator in a thermosyphon for the cooling of electronics shows significant promise.

In the present study, experiments were performed to investigate forced convection heat transfer in microcellular graphite foam of high thermal conductivity. The test section was designed to be adiabatic with a constant heat flux at the bottom channel. The graphite foam heat sinks were fabricated into different designed structures and compared with conventional aluminum heat sinks of the same configurations. The local temperature and Nusselt number distributions for steady flow through the tested heat sinks were measured. The results show that better heat transfer performance is obtained by graphite foam heat sinks as compared to the conventional aluminum heat sinks of different configurations. The graphite foam heat sink with a fin structure reaches the highest heat transfer rate among the tested heat sinks. The results imply that the advantage of isotropic thermal properties of graphite foam combined with open cell structure lends itself to novel designs in electronic cooling applications.

## NOMENCLATURE

$A_c$	[m <sup>2</sup> ]	cross sectional area of heat sinks
$A_h$	[m <sup>2</sup> ]	heated area
$D_h$	[mm]	hydraulic diameter of heat sinks
$h$	[W/m <sup>2</sup> ·K]	heat transfer coefficient
$k$	[W/m·K]	thermal conductivity
$k_f$	[W/m·K]	thermal conductivity of fluid
$Nu_x$	[-]	local Nusselt number
$Nu_l$	[-]	length averaged Nusselt number
$P_h$	[mm]	perimeter length of the heat sinks
$Q$	[W]	heating power
$Re$	[-]	Reynolds number
$T_{w,b}$	[°C]	local surface temperature
$T_{b,in}$	[°C]	inlet bulk temperature
$x$	[m]	axial distance along test section
$u$	[m/s]	mean flow velocity

### Special characters

$\mu$	[-]	dynamic viscosity of fluid
$\rho$	[kg/m <sup>3</sup> ]	density

### Subscripts

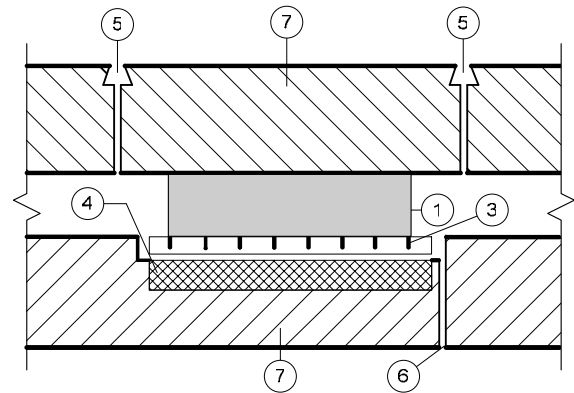
$b$	bulk
-----	------

$w$	wall
$x$	local position
$in$	inlet

## EXPERIMENTS

### Experimental Facility

To study forced convection in graphite foams and compare with conventional cooling media, experiments were performed using graphite foam and aluminum heat sinks of different configurations. The experiments of steady flow through the test section were facilitated by an auto-balance compressor. The air flow rate was adjusted by a flow regulator and a valve installed on the main line. Fig. 2 shows the cross sectional view of the test section. The test section is the tested heat sinks with dimensions of 50×50×10 mm. The channel was made of Teflon material and the channel was well insulated. A film heater was firmly mounted on the bottom of the channel to supply a constant heating power of 36 W, and a 1-mm thick copper plate with eight narrow slots perpendicular to the flow direction was attached on the surface of film heater. The copper plate was cleaned and eight thermocouples (K-type) were attached into eight narrow slots. To distribute the heat evenly on the copper plate and to reduce gap thermal resistance, thermal grease was used as a filling material between the heater and the copper plate. The other two thermocouples were placed at the inlet and outlet to measure the bulk temperatures. The flow velocity was measured by a hot-wire sensor which was mounted at the center of the channel. The two taps for the pressure sensors were located before and after the test section for pressure drop measurements.



1. Test heat sink 2. Copper plate 3. Slot 4. Film heater  
5. Pressure measuring tap 6. Thermocouple hole 7. Teflon

Fig. 2 Cross sectional view of the test section

### Heat Sink Configurations

Fig. 3 shows two configurations for the heat sinks tested in the present experiments, i.e. fins and holes structures. The graphite foam ( $k = 180$  W/m·K) and aluminum ( $k = 170$  W/m·K) heat sinks were made into the two structures as shown in Figs. 3(a) and (b), respectively. The hydraulic diameter of the heat sink  $D_h$  is defined as

$$D_h = \frac{4A_c}{P_h} \quad (1)$$

where  $A_c$  and  $P_h$  are the cross sectional area and perimeter length for heat sinks, respectively. The geometrical parameters of the designed heat sinks are listed in Table 1.

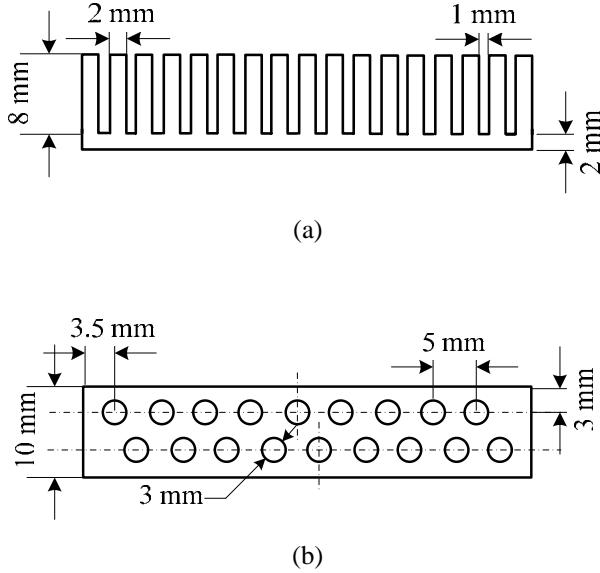


Fig. 3 Configurations of the tested heat sinks (a) fins structure (b) holes structure

Table 1 : Parameters of tested heat sinks in different configurations

	Fin structure	Hole structure
$A_c$	8 mm <sup>2</sup>	7.069 mm <sup>2</sup>
$P_h$	17 mm	9.425 mm
$D_h$	1.882 mm	3 mm

### Data Reduction

All temperature, velocity and pressure drop signals were acquired by a PC-based data acquisition system consisting of a voltage amplifier, pressure transducer, constant-temperature anemometer and a 12-bit A/D card within a personal computer. When a set of readings had been recorded, the test apparatus had to be cooled to ambient temperature of about 25°C before the next set of experiments can be started.

To minimize data reduction uncertainty, the time-averaged method was employed to reduce the data of steady flow experiments. The time-averaged local surface temperature is defined as the average temperature of local wall temperatures measured by thermocouple during a certain time under steady state conditions. The accuracies of the thermocouple temperature and pressure transducer readings are within  $\pm 0.1^\circ\text{C}$  and  $\pm 0.25\%$  of full-scale, respectively. The accuracy of the velocity measured by the hot-wire anemometer is  $\pm 0.01$  m/s. In the present experiments, the uncertainties of the measured data were assumed to be independent and random with normal distributions. After the time averaging process, uncertainties of

temperature, velocity and pressure are estimated to be 3.0 percent, 2.0 percent and 2.0 percent, respectively. The uncertainties of the calculated variables were determined by the method described by Taylor [15]. Details of the uncertainty analysis for the experimental data can be found in Refs. [6, 7].

### RESULTS AND DISCUSSION

Before the discussion of the experimental results, the dimensionless parameters used in the calculations were defined. The local Nusselt number for air flow through heat sinks is given by

$$Nu_x = \frac{h_x D_h}{k_f} \quad (2)$$

with

$$h_x = \frac{Q}{(T_{w,x} - T_{b,in})A_h} \quad (3)$$

where  $T_{w,x}$  is the temperature measured at the base of the heat sink and  $T_{b,in}$  is the bulk inlet temperature of air. The inlet bulk temperature used to calculate the local Nusselt number takes into consideration the thermal potential for heat transfer from the heated surface to the cold air. The Reynolds number based on the hydraulic diameter of the heat sink is given by

$$Re = \frac{\rho u D_h}{\mu} \quad (4)$$

where  $u$  and  $\mu$  are the mean velocity and dynamic viscosity of fluid flow, respectively.

### Temperature Distribution

Figs. 4(a) and (b) present the local temperature distributions along the flow direction on the substrate surface in graphite foam and aluminum finned heat sinks, respectively. From Fig. 4(a), it is observed that the local wall temperature in graphite foam heat sink increases with the increase of dimensionless axial position  $x/D_h$ . The temperatures decrease with increasing Reynolds number. The same trend of the temperature distribution for steady flow through aluminum finned heat sinks is found in Fig. 4(b). From a closer view of Fig. 4, it can be seen that the temperature profile of steady flow through graphite foam is lower than that of steady flow through aluminum finned heat sink at approximately the same Reynolds number. According to the data shown in Figs. 4(a) and (b), the average surface temperature for steady flow through graphite foam heat sink is 40.2°C at Reynolds number of 735. However, the average temperature on the substrate surface of aluminum heat sink is 56.5°C at an even higher Reynolds number of 809. The difference of the averaged temperature on the substrate surface between graphite foam and aluminum finned heat sinks is above 10°C for approximately the same Reynolds number.

Fig. 5 shows the local temperature distributions along the test section on the substrate surfaces in graphite foam and aluminum heat sinks with holes structure. It is obvious that the temperature profiles decrease with the increase of Reynolds number and increase along the flow direction for both graphite foam and aluminum heat sinks with holes configuration. Once again, it can be observed that the temperature profile of steady flow through graphite foam with holes structure is lower than

that of steady flow through aluminum heat sink at an approximately same Reynolds number. For Reynolds number of 1075, the average surface temperature on the graphite foam substrate surface is around 49°C. Comparatively, a higher average surface temperature of 54°C is obtained with an aluminum heat sink of the same configuration at a Reynolds number of 1003.

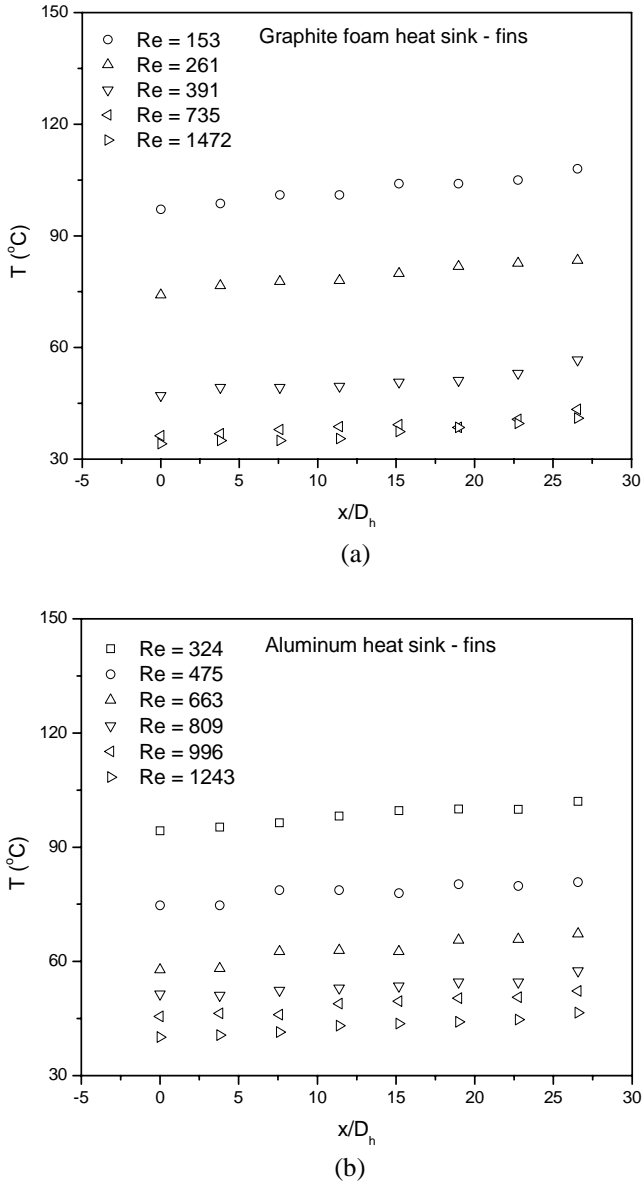


Fig. 4 Surface temperature distributions for air flow through (a) graphite foam (b) aluminum heat sinks with fins structure

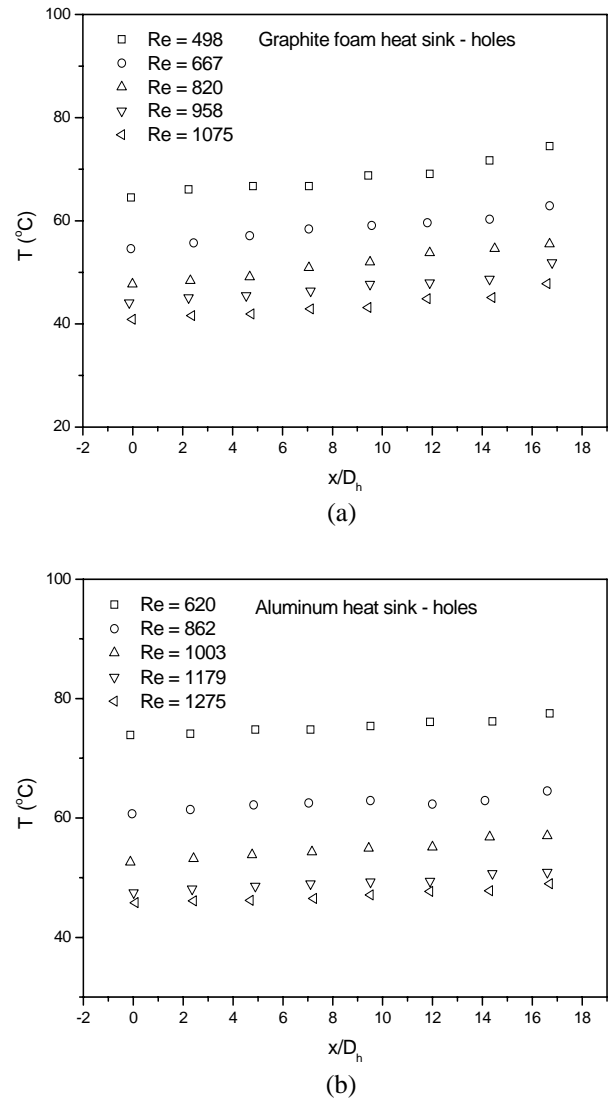


Fig.5 Surface temperature distribution for air flow through (a) graphite foam (b) aluminum heat sinks with holes structure

### Local Nusselt Number

Figs. 6(a) and (b) show the local Nusselt number distribution for steady flow through graphite foam and aluminum heat sinks with fins structure, respectively. It is seen that for both graphite foam and aluminum finned heat sinks, the local Nusselt number decreases along the test section at a given Reynolds number. The highest value of the local Nusselt number is obtained at the thermal entrance region. The fluctuation of the local Nusselt number for high Reynolds number is more significant as compared to that for low Reynolds number. It is also observed from Figs. 6(a) and (b) that the profile of the Nusselt number in graphite foam is higher than that in aluminum heat sinks at approximately the same Reynolds number. The local Nusselt numbers vary from 60 to 34 for steady flow through graphite foam at  $Re = 735$ . However, the local Nusselt numbers obtained vary from 40 to 29 for the aluminum heat sink at  $Re = 809$ .

The local Nusselt number distributions of steady flow

through graphite foam and aluminum heat sinks with holes structure are shown in Fig. 7. Overall, the same trend of the local Nusselt number distribution shown in Fig. 6 can be observed by heat sinks with holes structure, i.e. the Nusselt number decreases along the flow direction and the highest value of the local Nusselt number is achieved at the thermal entrance region. The graphite foam heat sink provides a higher Nusselt number profile as compared to the aluminum heat sink at approximately the same Reynolds number. For instance, the local Nusselt numbers vary from 64 to 43 at  $Re = 1075$  in the graphite foam and from 54 to 47 at  $Re = 1003$  in the aluminum heat sink. From the data of Figs. 6 and 7, it is found that variations of the local Nusselt numbers for graphite foam heat sinks are steeper than those for aluminum heat sinks. This is due to the porous structure of the tested graphite foams. The spherical pores with smaller openings between the cells inside the graphite foam heat sink generate fluid mixing which enhances further the heat transfer at the thermal entrance region.

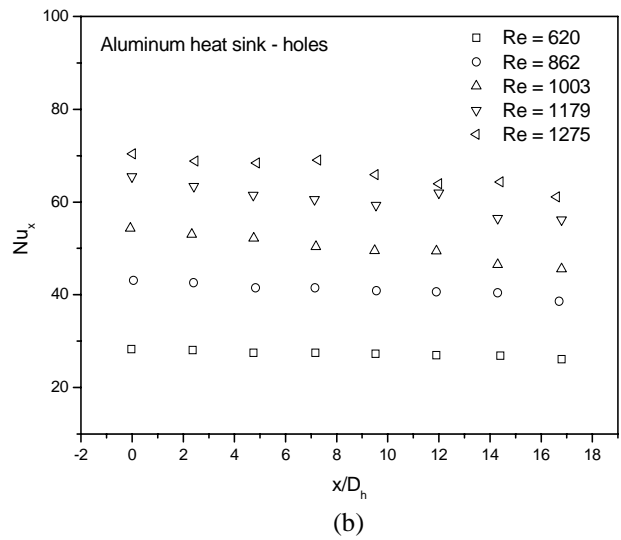
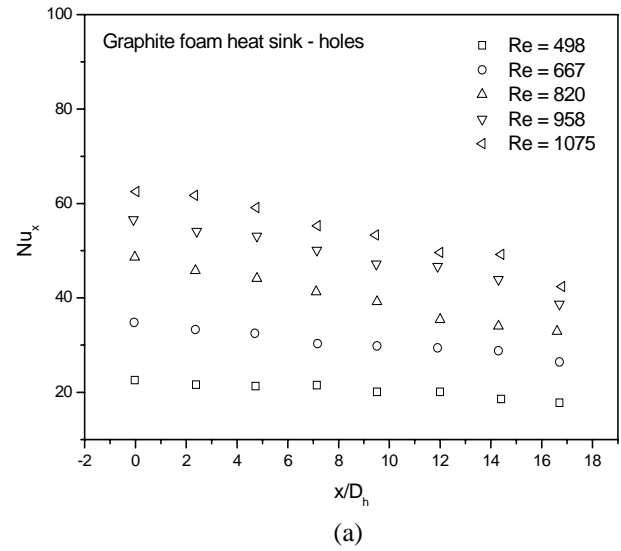


Fig. 7 Local Nusselt numbers for steady flow through (a) graphite foam (b) aluminum heat sinks with holes structure

**Total Heat Transfer Rate**

To evaluate the heat transfer performance for steady flow through the graphite foam and aluminum heat sinks, the length averaged Nusselt number is used to compare the total heat transfer in the tested materials. Fig. 8 shows the length averaged Nusselt number against Reynolds number for heat sinks of different configurations. The linear fitting lines of the length averaged Nusselt numbers for graphite foam and aluminum heat sinks (including fins and holes structures) show clearly that graphite foam material presents better heat transfer performance as compared to conventional aluminum material for the same flow conditions. It is observed that the graphite foam finned heat sink gives the highest length averaged Nusselt number within the range of Reynolds number. However, it is noted that the improvement of heat transfer in graphite foam with holes structure is not as significant as that in graphite foam

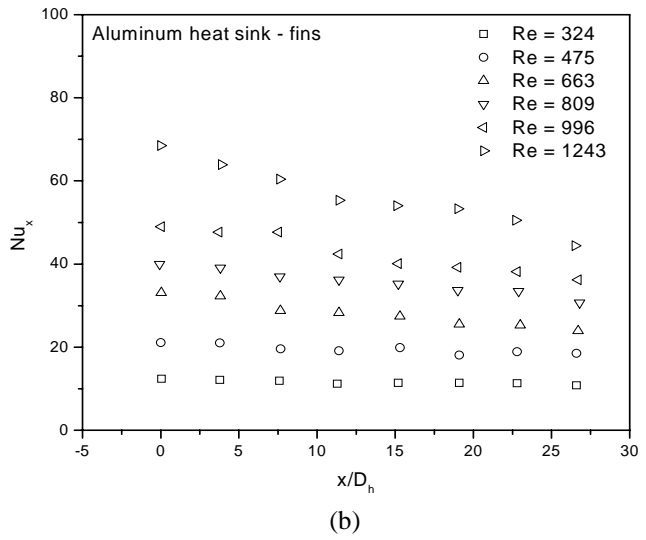
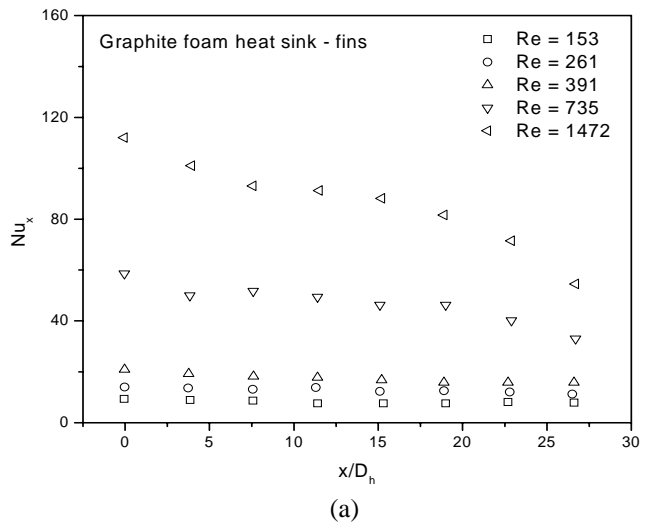


Fig. 6 Local Nusselt number for steady flow through (a) graphite foam (b) aluminum heat sinks with fins structure

with fins structure. According to the geometrical parameters of fins and holes structures shown in Table 1, the surface area of fins configuration is larger than that of holes configuration. The large surface area of finned graphite foam with small open cells can be considered as an extended fluid-to-solid contact area, which enhances the overall heat transfer.

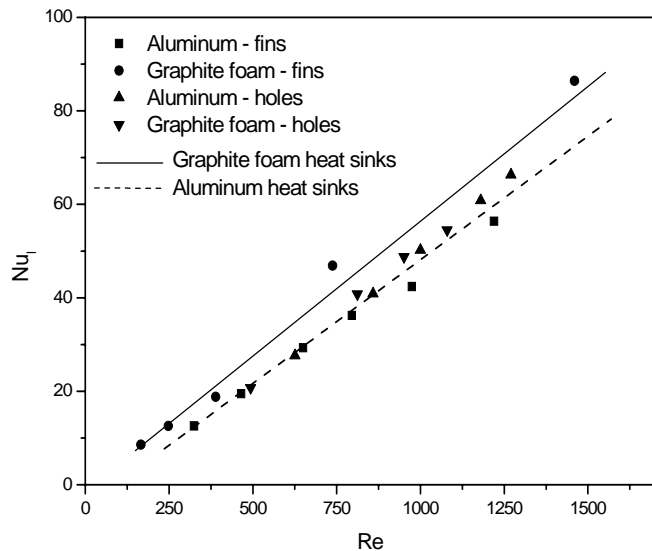


Fig. 8 Comparison of length averaged Nusselt numbers for steady flow through graphite foam and aluminum heat sinks

## CONCLUSION

An experimental investigation was performed to study the forced convection heat transfer in microcellular graphite foam of high thermal conductivity. Experiments were conducted based on a constant heat flux supplied at the bottom of the channel. Graphite foam heat sinks with fins and holes structures were tested and compared to conventional aluminum heat sinks of the same configurations. It is found that the local temperatures increase along the test section and decrease with Reynolds number, while the Nusselt number distributions exhibit the opposite trend. The results show that better heat transfer performance are obtained by graphite foam heat sinks as compared to conventional aluminum heat sinks due to the porous structure, which enhances heat transfer at the thermal entrance region. The graphite foam heat sink with fin structure achieves the highest heat transfer rate among the tested heat sinks. The results imply that the advantage of isotropic thermal properties of graphite foam combined with open celled structure lends itself to novel designs in electronic cooling applications.

## ACKNOWLEDGMENTS

This work is supported financially in part by the Defence Science and Technology Agency, Singapore through Grant no. DSTA-NTU-DIRP/2005/01. The authors gratefully acknowledge the assistance of Mr. Elvin Teh for his meticulous collection of experimental data for the results presented in this paper.

## REFERENCES

- [1] Viswanath, R., Wakharkar, V., Watwe, A., and Lebonheur, V., Thermal performance challenges from silicon to systems, *Intel Technology Journal*, Vol. 3, 2000, pp. 1-16.
- [2] Azar, K., and Morabito, J., Managing power requirements in the electronics industry, *Electronics Cooling*, Vol.6, No.4, 2000, pp. 12-25.
- [3] Bhattacharya, A., and Mahajan, R.L., Finned metal foam heat sinks for electronics cooling in forced convection, *ASME Journal of Electronic Packaging*, Vol. 124, 2002, pp. 155-163.
- [4] Boomsma, K., Poulidakos, D., and Zwick, F., Metal foams as compact high performance heat exchangers, *Mechanics of Materials*, Vol. 35, 2003, pp. 1161-1176.
- [5] Fu, H.L., Leong, K.C., Huang, X.Y., and Liu, C.Y., An experimental study of heat transfer of a porous channel subjected to oscillating flow, *ASME Journal of Heat Transfer*, Vol. 123, 2001, pp. 162-170.
- [6] Leong, K.C., and Jin, L.W., An experimental study of heat transfer in oscillating flow through a channel filled with an aluminum foam, *International Journal of Heat and Mass Transfer*, Vol. 48, 2005, pp. 243-253.
- [7] Leong, K.C., and Jin, L.W., Effect of oscillatory frequency on heat transfer in metal foam heat sinks of various pore densities, *International Journal of Heat and Mass Transfer*, Vol. 49, 2006, pp. 671-681.
- [8] Klett, J.W., High thermal conductivity mesophase pitch-derived graphitic foams, *Composites in Manufacturing*, Vol. 14, 1999, pp. 123-129.
- [9] Gallego, N.C., and Klett, J.W., Carbon foams for thermal management, *Carbon*, Vol. 41, 2003, pp. 1461-1466.
- [10] Klett, J.W., Mcmillan, A.D., Gallego, N.C., and Walls, C.A., The role of structure on the thermal properties of graphitic foams, *Journal of Materials Science*, Vol. 39, 2000, pp. 3659-3676.
- [11] Ott, R.D., Zaltash, A., and Klett, W.J., Utilization of a graphite foam radiator on a natural gas engine-driven heat pump, *Proceedings of IMECE 2002 ASME International Mechanical Engineering Conference and Exposition*, Louisiana, USA, 2002.
- [12] Yu Q.J., Straatman, A.G., and Thompson, B.E., Carbon-foam finned tubes in air-water heat exchangers, *Applied Thermal Engineering*, Vol. 26, 2006, pp. 131-143.
- [13] Druma, A.M., Alam, M.K., and Druma, C., Analysis of thermal conduction in carbon foams, *International Journal of Thermal Sciences*, Vol. 43, 2004, pp. 689-695.
- [14] Coursey, J.S., Kim, J., and Boudreaux, P.J., Performance of graphite foam evaporator for use in thermal management, *ASME Journal of Electronic Packaging*, Vol. 127, 2005, pp. 127-134.
- [15] Taylor, J.R. *An Introduction to Error Analysis – Study of Uncertainty in Physical Measurements*, Oxford University Press, 1995.